JOURNAL OF VIROLOGY, Feb. 2010, p. 1752–1763 Vol. 84, No. 4
0022-538X/10/$12.00 doi:10.1128/JVI.01758-09

The Murine Coronavirus Nucleocapsid Gene Is a Determinant of Virulence▽

Timothy J. Cowley, Simon Y. Long,† and Susan R. Weiss*

Department of Microbiology, University of Pennsylvania School of Medicine, Philadelphia, Pennsylvania 19104

Received 20 August 2009/Accepted 25 November 2009

The murine coronavirus, mouse hepatitis virus (MHV) strain A59, causes acute encephalitis and chronic demyelinating disease as well as hepatitis in mice. The JHM strain (also called MHV-4 or JHM.SD) causes fatal encephalitis and only minimal hepatitis. Previous analysis of chimeric recombinant MHVs in which the spike gene, encoding the protein that mediates viral entry and cell-to-cell fusion, was exchanged between JHM and A59 showed that the spike plays a major role in determining organ tropism and neurovirulence but that other genes also play important roles in pathogenic outcome. Here, we have investigated the role of the nucleocapsid protein in MHV-induced disease. The multifunctional nucleocapsid protein is complexed with the genomic RNA, interacts with the viral membrane protein during virion assembly, and plays an import role in enhancing the efficiency of transcription. A pair of chimeric recombinant viruses in which the nucleocapsid gene was exchanged between JHM and A59 was selected and compared to wild-type parental strains in terms of virulence. Importantly, expression of the JHM nucleocapsid in the context of the A59 genome conferred increased mortality and spread of viral antigen in the mouse central nervous system compared to the parental A59 strain, while having little effect on the induction of hepatitis. While the JHM nucleocapsid did not appear to enhance neuron-to-neuron spread in primary neuronal cultures, the increased neurovirulence it conferred may be due in part to the induction of a less robust T-cell response than that induced by strain A59.

Coronaviridae are a family of large, single-stranded and positive-sense RNA viruses within the nidovirus superfamily. The murine coronavirus mouse hepatitis virus (MHV) is a collection of strains with a wide range of tropisms, inducing neurological, hepatic, enteric, and respiratory diseases, with outcomes dependent upon the viral strain and the route of infection. Infection via intracranial (i.c.) or intranasal (i.n.) routes serves as a model for studying both acute and chronic virus-induced neurological diseases; these include models of encephalitis and the demyelinating disease multiple sclerosis. Two naturally occurring neurotropic strains, A59 and JHM, have been shown to induce very different pathologies following i.c. infection. The A59 strain is a weakly neurovirulent, tissue culture-adapted strain that induces mild encephalitis and moderate hepatitis (20, 40). A59 infection is cleared from the central nervous system (CNS) and liver following a robust CD8 T-cell response (24, 49) (22); however, viral RNA persists in the spinal cord, and chronic demyelination develops in animals surviving acute infection (12, 19, 26) In contrast, the JHM strain, which has been previously referred to as MHV-4 or JHM.SD (5, 36), is highly neurovirulent in weanling C57BL/6 (B6) mice, inducing fatal encephalitis in nearly all infected mice following inoculation with doses as low as 1 PFU. This enhanced virulence is attributed in part to its rapid spread in the CNS, which occurs by MHV receptor CEACAM1a-dependent and -independent mechanisms (28), and likely also to the lack of a robust CD8 T-cell response in the CNS (21).

We have previously selected chimeric A59/JHM recombinant viruses, which have been used to define the roles of both spike (S) and background genes in CNS pathogenesis. The S gene, encoding the protein responsible for attachment to the host cell and subsequent fusion and entry, as well as for cell to cell spread, is clearly a major determinant of MHV neurovirulence. Replacement of the S gene of A59 with that of JHM (S_{JHM}) confers upon the recombinant A59 (rA59) virus a highly neurovirulent phenotype. This chimeric virus, rA59/S_{JHM} is characterized by a 3-$\log_{10}$ decrease in the intracranial 50% lethal dose (LD_{50}), increased rate of viral antigen spread, and increased inflammation compared with wild-type rA59 (15, 23, 40). However, this chimeric virus is less neurovirulent than the wild-type recombinant JHM (rJHM) virus, likely due at least in part to the induction of a robust CD8 T-cell response (21, 15). Furthermore, unlike rJHM, rA59/S_{JHM} induces hepatitis when inoculated at a high dose (31). Further analysis of additional A59/JHM chimeric viruses, including the reverse chimeric virus rJHM/S_{A59} (where the S gene of JHM has been replaced by that of A59) (31) and viruses with exchanges of 5′ replicase gene portions of the genome (32), demonstrated that, in addition to S, one or more genes within the 3′ end of the JHM genome are necessary for the extremely high neurovirulence of JHM.

The nucleocapsid protein (N), encoded in the most-3′ gene of the MHV genome, plays several roles in infection. N is a basic RNA binding protein (1, 47) that plays structural roles by both complexing with genome RNA to form the viral capsid (48) and interacting with the viral membrane protein (M) during virion assembly (14). In addition, N has several other functions during replication. Nucleocapsid protein (i) associ-

* Corresponding author. Mailing address: Department of Microbiology, University of Pennsylvania, School of Medicine, 36th Street and Hamilton Walk, Philadelphia, PA 19104-6076. Phone: (215) 898-8013. Fax: (215) 573-4858. E-mail: weisssr@mail.med.upenn.edu.

† Present address: Department of Molecular and Comparative Pathobiology, Johns Hopkins University School of Medicine, Baltimore, MD 21205.

▽ Published ahead of print on 9 December 2009.

ates with genomic and subgenomic mRNA (2); (ii) significantly enhances recovery of infectious virus from transfected genome-length synthetic RNA (2, 52); (iii) has been reported to associate with microtubules (39), suggesting a possible role for N in trafficking and axonal transport in neurons; and (iv) has been shown to antagonize type I interferon (IFN) by blocking RNase L activity (51). Furthermore, N proteins from A59 and a highly hepatotropic strain, MHV-3, but not JHM were shown to be responsible for the induction of fibrinogen-like protein 2 (fgl2), a multifunctional protein that has both procoagulant and immunosuppressive activities and leads to enhanced liver damage during MHV infection (6, 27, 35). Finally, N is unique among MHV structural proteins in that it is partially localized to the nucleus of infected cells (50).

N protein has three conserved regions (I, II, and III) separated by two hypervariable regions (A and B) (38). Crystal structures of the related infectious bronchitis virus (IBV) and severe acute respiratory syndrome coronavirus (SARS-CoV) N show that N has two structured domains designated the N-terminal domain (NTD), beginning within conserved region I and ending within conserved region II, and the C-terminal domain (CTD), residing within conserved region II and ending before the hypervariable region B (7, 13, 17, 46, 53). Conserved region II is involved in RNA binding (25, 34) while conserved region III is involved in M binding (14). The N protein is highly conserved among MHV strains. Sequence analysis reveals 94% identity at the amino acid level between the N proteins of A59 and JHM and 28 amino acid differences, 11 of which are outside of the hypervariable regions. We have selected chimeric recombinant viruses in which the N gene alone or in combination with the S gene has been exchanged between A59 and JHM. These chimeric viruses have been used to investigate the role of N in virulence.

MATERIALS AND METHODS

Cells and viruses. Murine fibroblast (L2 and 17Cl-1) cells and feline *Felis catus* whole fetus (FCWF) cells were maintained in Dulbecco's minimal essential medium supplemented with 10% fetal bovine serum (FBS), 1% amphotericin B (Fungizone), 10 mM HEPES, and 2 mM L-glutamine. Primary neuronal cultures were generated from hippocampal tissue harvested from day 15 to 16 embryonic mice. Neurons were grown on poly-L-lysine-treated glass coverslips and cultured at 37°C with 5% CO_2 in neurobasal medium (Gibco) containing B27 supplement (Gibco). Neurons were allowed to differentiate for 4 days prior to infection (41).

Previously described viruses include the following: (i) wild types rA59 (40) and rJHM (31) and (ii) S exchange viruses rA59/S_{JHM} (40) and rJHM/S_{A59} (31). Chimeric viruses with exchanges of N genes (rA59/N_{JHM} and rJHM/N_{A59}) or N and S genes (rA59/S_{JHM}/N_{JHM} and rJHM/S_{A59}/N_{A59}) were selected by targeted recombination as described below. Recombinant viruses were propagated on mouse 17Cl-1 cells; plaque assays and plaque purification of recombinants were carried out on L2 cells (11). Wild-type rA59 and rJHM were indistinguishable in phenotype from their parental wild type (5, 23, 31, 40).

Please note that we have changed our previously used nomenclature in an effort to make it simpler and more logical. Recombinant viruses are labeled "r" for recombinant, followed by the strain from which the background genes are derived, followed by the strain of the genes that have been replaced. For example, rA59/S_{JHM} is a recombinant A59 expressing the JHM S; this virus was previously called SJHM/RA59. rJHM/S_{A59} was previously called SA59/RJHM.

Plasmids. For the selection of chimeric viruses of the A59 background, the plasmid pMH54 was utilized. pMH54 contains the 3′ third of the A59 genome, from codon 48 of the hemagglutinin esterase (HE) gene through the 3′ end of the genome (18). pSG6, a modification of pMH54, contains two silent point mutations at nucleotides 8838 and 8841, which generate a unique BspEI site after codon 444 of the N gene (10). This plasmid was kindly provided by Paul Masters.

The N gene of pSG6 was exchanged for that of JHM to create pSG6/N_{JHM}, the plasmid from which rA59/N_{JHM} was generated. Specifically, a fragment containing nucleotides 7529 to 9003 was amplified from pJHM (37) using PCR, *Pfu* polymerase, and primers that created 5′ BssHII and 3′ BspEI sites. The resulting fragment (beginning at codon 187 of the M gene and ending codon 445 of the N gene) spanning a conserved region of M and containing all the coding differences between the A59 and JHM N genes was cloned into pSG6, using unique 5′ BssHII and 3′ BspEI sites, to create pSG6/N_{JHM}. For selection of rA59/S*JHM*/N_{JHM}, the A59 S gene was replaced by the JHM S gene using AvrII and SbfI sites as described previously (40).

The plasmid pJHM, analogous to pMH54, contains the 3′ portion of the JHM genome (37) and was used to generate JHM background viruses. For selection of rJHM/N_{A59}, pJHM was modified to create pJHM/N_{A59}, by exchanging the N gene for that of A59 derived from pSG6. Thus, a silent mutation was introduced at nucleotide 7531 of pJHM to create a BssHII site at codon 187 of the M gene (corresponding to a site found in pMH54). PCR was then used to generate a fragment from nucleotide 7367 to 8898 of pSG6, which begins at codon 187 of the M gene and ends in the 3′ untranslated region 30 nucleotides after the end of the N gene. Primers used to amplify this region contained a 5′ BssHII site and created a 3′ DraIII site, corresponding to a site present in pJHM. The BssHII and DraIII sites were used to clone the fragment into pJHM, creating pJHM/N_{A59}. pJHM/N_{A59} was further modified to create pJHM/S_{A59}/N_{A59} by exchanging the S genes using the AvrII and SbfI sites, as described above (40).

Selection of recombinant viruses. Targeted recombination was carried out as described previously (18, 40). Briefly, FCWF cells were infected with fMHV-A59, a virus expressing the feline infectious peritonitis virus (FIPV) S within the A59 background, or with fMHV-JHM, a virus expressing FIPV S in the JHM background. RNAs transcribed *in vitro* from the chimeric plasmids described above were electroporated into infected FCWF cells, and infected transfected FCWF cells were overlaid onto confluent murine 17Cl-1 cells. Viruses were selected for their ability to infect murine cells and were plaque purified twice on L2 cells. At least two viruses of each genotype, isolated from independent recombination events, were plaque purified, and the S and N genes were sequenced. There were no differences observed between the *in vitro* and *in vivo* phenotypes of the two viruses of each genotype. Thus, we will show the data for one of each genotype virus.

Virus growth curves. Confluent monolayers of L2 cells were infected at a multiplicity of infection (MOI) of 1. At the times indicated in the figures, the cells and supernatants were lysed by three freeze-thaw cycles, and debris was removed by centrifugation. Titers of lysates were then determined by plaque assay of L2 cells as previously described (11).

Neuronal cultures, infections, and quantification. Primary hippocampal neuronal cultures, as described above, were infected with the viruses indicated in the figure legends at a MOI of 1 or left uninfected. At days 1 to 4 postinfection, cultures were fixed in a solution of 2% paraformaldehyde in phosphate-buffered saline (PBS) containing 0.12 M sucrose and stored in PBS at 4°C until staining. Fixed neurons were stained with antinuclecocapsid (anti-N) monoclonal antibody (MAb) 1.16.1 (kindly provided by J. Leibowitz, Texas A&M University) using a Vector ABC immunoperoxidase kit (Vector, Burlingame, CA). Cells were counterstained with either hematoxylin or methyl green. Quantification of the area of individual foci was carried out using the color cube-based segmentation function of Image Pro, version 5.0, software.

***In vivo* infections. (i) Mice and inoculations.** Pathogen-free 4- to 5-week-old male C57BL/6 mice were obtained from NCI (Fredrick, MD). All experiments were performed in containment within a biosafety level 2 animal facility and conducted in accordance with the guidelines of the Institutional Animal Care and Use Committee (IACUC) at the University of Pennsylvania.

(ii) Virulence assays. Virus was serially diluted 10-fold with PBS containing 0.75% bovine serum albumin. Mice (5 to 10 per viral dose) were anesthetized with isoflurane and inoculated in the left cerebral hemisphere with virus. Mice were monitored daily for 21 days and euthanized when they became moribund and counted along with mice found dead the following day. Statistical comparison of survival curves was performed using a Gehan-Breslow-Wilcoxon test, and LD_{50} values were calculated (42).

Virus replication *in vivo*. (i) Brain. Mice were infected i.c. with 50 PFU of virus and on day 5 postinfection were sacrificed and perfused with 10 ml of PBS. The brains were removed and cut in half along the midline. The right halves were fixed in formalin to be used for histology as described below and the left halves were placed in 2 ml of isotonic saline containing 0.167% gelatin, weighed, and stored at −80°C for virus titration. Brains were homogenized, and virus titers were determined by plaque assay as described previously (11). Statistical comparisons were made using a two-tailed *t* test.

(ii) Liver. Mice were infected intrahepatically (i.h.) with 500 or 1.6×10^4 to 1.8×10^4 PFU of virus as described previously (30). Five days postinfection mice were sacrificed and perfused with PBS. Livers were harvested and homogenized, and titers

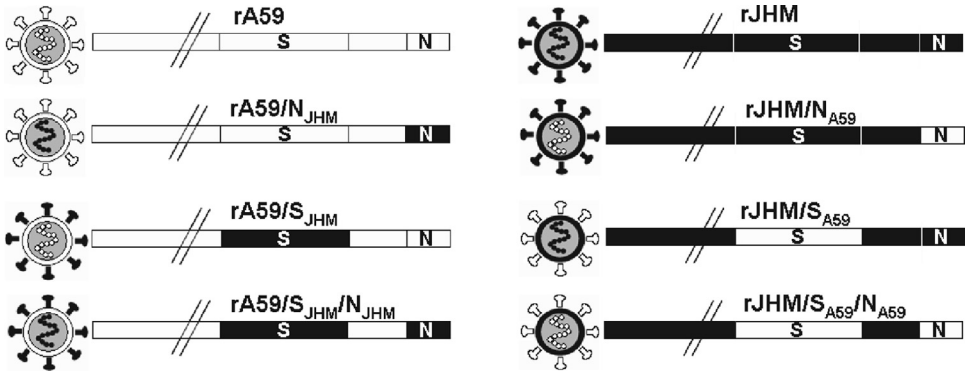

FIG. 1. Schematic representation of the virions and corresponding genomes of recombinant viruses. Shown on the left are A59 background viruses and, on the right, the JHM background viruses. A59 components are in white, and JHM components are in black. The positions of the spike (S) and nucleocapsid (N) genes are noted. The 5′ replicase gene is not shown to scale, as indicated by hash marks.

of lysates were determined for infectious virus as described above. Statistical comparisons were made using a two-part two-tailed *t* test.

Histology, immunohistochemistry, and quantification of viral antigen. Formalin-fixed brains, harvested from mice sacrificed at 5 days postinfection, were paraffin embedded and sectioned sagitally. Viral antigen was detected using anti-N MAb 1.16.1 and the Vector ABC immunoperoxidase kit, as previously described (30). Sections were counterstained with hematoxylin. Pictures taken of each stained brain section were analyzed using the color cube-based segmentation function of Image Pro, version 5.0, software to calculate total stained area and total area of each section. The ratio of stained area to total section area was used as a means of quantifying the amount of viral antigen staining in each section. Five or more mice were used per group, with two adjacent sections per mouse. A two-tailed *t* test was used to determine significance.

Histology, immunohistochemistry, and quantification of antigen for the liver sections were carried out using the same methodology as above, utilizing a section of the median liver lobe cut about 0.5 cm from the tip. Hepatitis was scored by examining liver sections stained with hematoxylin and eosin. Sections were evaluated for degree of inflammation and necrosis and scored on a four point scale (4, severe; 3, moderate; 2, mild; 1, minimal; 0, none) as previously described (3, 31).

Isolation of brain mononuclear cells. Mice were infected either i.c. with 10 PFU of virus or i.n. with 500 PFU of virus. Seven days postinfection, the peak of T-cell response in the brain, mice were perfused, and brains were harvested (22). Brains were placed in RPMI medium containing 10% FBS and homogenized through a nylon mesh bag (pore diameter, 64 μm) with moderate pressure from a syringe plunger. Cells were then passed through a 30% Percoll gradient and through a cell strainer (pore diameter, 70 μm) and then washed and counted.

T-cell quantification. Up to 1×10^6 brain-derived mononuclear cells were analyzed per brain. Cells were stained for surface expression of CD3, CD8, and CD4 using fluorescently conjugated monoclonal antibodies (BD Pharmingen) (peridinin chlorophyll protein [PerCP]-conjugated CD3ε, clone 145-2C11; fluorescein isothiocyanate [FITC]-conjugated CD8α, clone 53-6.7; phycoerythrin [PE]-conjugated CD4, clone GK1.5) and stained for T-cell receptors specific for the major CD8 epitope, S510, using allophycocyanin (APC)-conjugated major histocompatibility complex (MHC) tetramers (kindly provided by Stanley Perlman, University of Iowa). Cells were fixed in 2% paraformaldehyde and analyzed using a FACSCalibur flow cytometer (Becton Dickinson). Total cell numbers per mouse were determined by multiplying the fraction of live cells positive for a given marker by the total number of live cells isolated. CD8 T cells were defined as those cells of lymphocyte size based on forward and side scatter that expressed CD3 and CD8 but lacked CD4 expression. S510-specific T cells were those within the CD8 T-cell population that were stained by the S510 tetramer. CD4 T cells were defined as those cells of lymphocyte size that expressed CD3 and CD4 but lacked CD8 expression.

For quantification by intracellular IFN-γ staining assay, similar methodology was used as above except that peptide incubation and intracellular IFN-γ staining steps were added in place of the MHC tetramer staining (29, 41), and CD3 staining was omitted. Thus, cells were cultured with 10 U of human recombinant interleukin-2 and 1 μl/ml brefeldin A (Golgiplug; BD Biosciences) in the presence of 1 μg/ml of peptide corresponding to the subdominant CD8 T-cell epitope, S598, in RPMI 1640 medium supplemented with 5% FBS for 5 h at 37°C. Cells were then stained for the surface expression of CD4 and CD8. These cells were then fixed and permeabilized using a Cytofix/Cytoperm kit (BD Biosciences) and stained for IFN-γ with an FITC-conjugated monoclonal antibody (BD Pharmingen).

RESULTS

Selection and *in vitro* characterization of A59/JHM chimeric recombinant viruses with exchanges of nucleocapsid genes. Previous analyses of chimeric A59/JHM recombinant viruses have shown that the differences in pathogenesis between the highly neurovirulent JHM and the weakly neurovirulent but hepatotropic A59 strains are in part attributed to the S gene. However, it is clear that the extremely high neurovirulence of JHM, the inability of JHM to induce a robust CD8 T-cell response, and the inability of JHM to induce hepatitis are influenced by other genes encoded within the 3′ third of the genome, which includes the structural genes envelope (E), membrane (M), nucleocapsid (N), and internal (I) and the putative nonstructural genes ORF4 and ORF5a (15, 31, 33). Because of the multiple functions of N both as a structural protein and in replication, we have investigated its contributions to pathogenesis. Targeted recombination was used to select isogenic viruses differing only in the N gene. More specifically, we selected A59 background viruses in which the A59 N gene was replaced with that of JHM (rA59/N$_{JHM}$). We also selected the reverse JHM background viruses, replacing the N gene of JHM with that of A59 (rJHM/N$_{A59}$) (Fig. 1). To investigate to what extent phenotypic differences between JHM and A59 can be explained by S and N together, a second set of chimeric viruses was selected in which both the S and N genes were exchanged (Fig. 1). Also shown in Fig. 1 are representations of the genomes of previously described recombinants in which S genes have been exchanged (31).

To verify that the chimeric viruses replicate efficiently in tissue culture and to determine if the genotype of N has an effect on replication patterns, rA59/N$_{JHM}$ and rJHM/N$_{A59}$ were compared to parental wild-type rA59 and rJHM in one-step growth curves (Fig. 2A). As previously reported, rJHM replicates with significantly slower kinetics and to a lower titer than rA59 in tissue culture (40). The N exchange viruses replicated with similar kinetics as their respective parental viruses

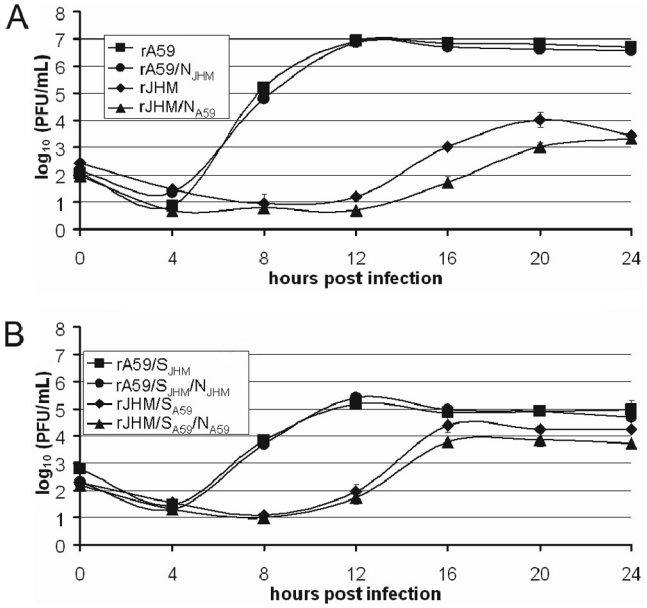

FIG. 2. Replication of recombinant viruses. L2 cells were infected (in duplicate) at an MOI of 1 with wild-type (A) and N exchange viruses or with S exchange viruses with and without N exchange (B). At the times indicated, virus was harvested from combined supernatants and cells, and titers were determined on L2 cell monolayers as described in Materials and Methods. Duplicate samples were averaged. The data are from one representative experiment of two.

although rJHM/N$_{A59}$ replicated slightly less efficiently than rJHM (Fig. 2A). Similarly, one-step growth curves were performed using rA59/S$_{JHM}$/N$_{JHM}$ and rJHM/S$_{A59}$/N$_{A59}$ and their parental controls rA59/S$_{JHM}$ and rJHM/S$_{A59}$ (Fig. 2B). As previously reported, the *in vitro* replication patterns of chimeric viruses segregated with the S gene (40). Importantly, exchange of the N genes did not alter either the kinetics of replication or the final extent of replication *in vitro* (Fig. 2B). These data indicate that these chimeric recombinants are not impaired in the ability to replicate *in vitro*. In addition, plaques of chimeric viruses were similar in size and shape to the corresponding isogenic parental viruses (data not shown).

JHM nucleocapsid protein is a determinant of high neurovirulence. rA59 and rJHM, like the wild-type isolates from which they were derived, display strikingly different levels of virulence in the CNS (15, 23). Intracranial (i.c.) infection with less than 10 PFU of rJHM typically kills all infected mice. In contrast, i.c. infection with rA59 requires approximately 3×10^3 to 5×10^3 PFU to kill half the mice (15, 23). JHM S greatly contributes to this difference as rA59/S$_{JHM}$ also kills mice with fewer than 10 PFU (15, 23, 40). The rJHM-infected mice, however, die more quickly than the rA59/S$_{JHM}$-infected mice, with the mean survival time being about 2 days less for JHM-infected mice (15). To determine if JHM N contributes to high neurovirulence, weanling C57BL/6 mice were infected i.c. (at the doses indicated in Fig. 3) with rA59/N$_{JHM}$ and rJHM/N$_{A59}$ and their parental viruses rA59 and rJHM. Mice were observed daily for illness and mortality; survival times were recorded,

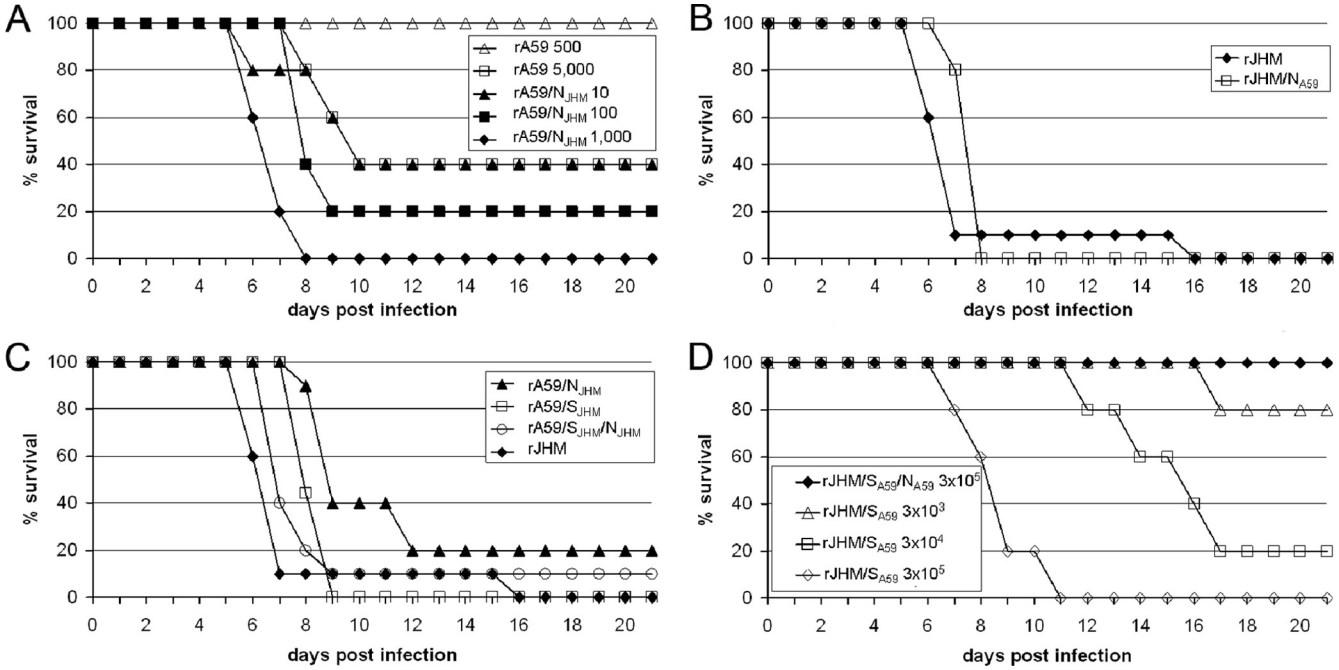

FIG. 3. Survival curves of infected 4-week-old C57BL/6 mice. Mice were infected with recombinant viruses at the doses indicated and observed over 21 days for mortality. (A) Infection with rA59 (500 PFU and 5×10^3 PFU) and rA59/N$_{JHM}$ (10 PFU, 100 PFU, and 1×10^3 PFU). rA59/N$_{JHM}$ at a dose of 100 PFU is significantly more virulent than rA59 at a dose of 500 ($n = 5$ each; $P = 0.0155$). (B) Infection with rJHM and rJHM/N$_{A59}$ at 10 PFU. rJHM/N$_{A59}$ is significantly less virulent than rJHM ($n = 10$ and 5, respectively; $P = 0.0272$). (C) Infection with rJHM, rA59/N$_{JHM}$, rA59/S$_{JHM}$, and rA59/S$_{JHM}$/N$_{JHM}$ (10 PFU). rA59/S$_{JHM}$/N$_{JHM}$ is more virulent than rA59/N$_{JHM}$ ($n = 10$ each; $P = 0.0030$) and rA59/S$_{JHM}$ ($n = 10$ and 9, respectively; $P = 0.0016$), and rJHM is more virulent than rA59/S$_{JHM}$/N$_{JHM}$ ($n = 10$ each; $P = 0.0319$). (D) Infection with rJHM/S$_{A59}$/N$_{A59}$ (3×10^5 PFU) and rJHM/S$_{A59}$ (3×10^3 PFU, 3×10^4 PFU, and 3×10^5 PFU). rJHM/S$_{A59}$ is more virulent than rJHM/S$_{A59}$/N$_{A59}$ ($n = 5$ each; $P = 0.0041$). The data are from one representative experiment of two or more.

TABLE 1. LD_{50} values

Virus	LD_{50} (PFU)
rA59	7.7×10^3
rA59/N_{JHM}	<10
rA59/S_{JHM}	<10
rA59/S_{JHM}/N_{JHM}	<10
rJHM	<10
rJHM/N_{A59}	<10
rJHM/S_{A59}	9.5×10^3
rJHM/S_{A59}/N_{A59}	>3.0×10^5

and LD_{50} values were calculated. Consistent with previous observations, rA59 was not lethal at a dose of 500 PFU (Fig. 3A) and the LD_{50} averaged 7.7×10^3 (Table 1). In contrast, infection of mice with only 10 PFU of rA59/N_{JHM} killed 60 to 80% (Fig. 3A and C) of mice, and the survival curve was similar to that of infection with 5×10^3 PFU of rA59 (Fig. 3A). The LD_{50} for rA59/N_{JHM} was <10 PFU, 100- to 1,000-fold less than that of rA59 and similar to that of rJHM (Table 1). Thus, expression of JHM N within the rA59 background enhances neurovirulence significantly. Conversely, expression of A59 N from within the rJHM background (rJHM/N_{A59}) decreased neurovirulence to a slight extent compared with rJHM (Fig. 3B). This difference is difficult to measure, probably because of the very high virulence (LD_{50} of <10 PFU) of both of these viruses.

To determine to what extent the neurovirulence differences between A59 and JHM can be explained by a combination of the N and S genes, mice were infected with chimeric viruses (rA59/S_{JHM}, rA59/N_{JHM}, rA59/S_{JHM}/N_{JHM}, rJHM/S_{A59}, and rJHM/S_{A59}/N_{A59}) and the parental rA59 and rJHM at the doses specified in Fig. 3. As previously observed, rA59/S_{JHM} is highly lethal at 10 PFU, which indicates that it is significantly more virulent than rA59 (Fig. 3C) (15, 40). Infection with a virus expressing both the JHM S and N genes within the rA59 background (rA59/S_{JHM}/N_{JHM}) was highly lethal, resulting in survival kinetics close to that of rJHM (Fig. 3C). Expression of the A59 S in the JHM background increased the LD_{50} to a value similar to that of rA59, which in this experiment was 9.5×10^3 PFU for rJHM/S_{A59} and 1.2×10^4 PFU for rA59 (Fig. 3D). Interestingly rJHM/S_{A59}/N_{A59} was nonlethal even at the very high dose of 3×10^5 PFU, indicating that replacing the JHM N gene with that of A59 is attenuating (Fig. 3D and Table 1). rA59 when expressing JHM S and N closely resembles rJHM in terms of virulence, but expressing both A59 S and N in the rJHM background attenuates the virus beyond the level of A59.

Replication and spread of recombinant viruses in the CNS. Despite vastly different levels of neurovirulence, wild-type and A59/JHM spike exchange chimeric recombinants replicate to similar levels in the brain during the first week postinfection, with titers and viral antigen levels peaking at day 5 (31, 40). Differences in neurovirulence are reflected in the extent of viral antigen detected in the brain, with rJHM-infected mice displaying extensive antigen spread compared to rA59-infected mice and with chimeric rA59/S_{JHM}-infected mice displaying an intermediate level, consistent with neurovirulence as described above (15, 23, 41) (Fig. 3C). Thus, we compared both virus titer and extent of viral antigen expression in the brains of mice infected with wild-type chimeric recombinant viruses at day 5 postinfection. Mice were infected with 50 PFU of chimeric viruses rA59/N_{JHM} and rJHM/N_{A59} and parental viruses rA59 and rJHM. At 5 days postinfection, brains were harvested and titrated for infectious virus by plaque assay. All viruses replicated to high titers in the brain (Fig. 4). However, exchange of the N genes appeared to affect replication in the brain, as demonstrated by a slight, but reproducibly significant, increase in rA59/N_{JHM} replication over rA59 ($P = 0.0001$) (Fig. 4) and a similarly small decrease in replication of rJHM/N_{A59} compared to rJHM ($P = 0.0128$) (Fig. 4).

To determine the extent of virus spread in the brain at the peak of acute infection, a consistent correlate of neurovirulence, mice were infected with 50 PFU of rA59/N_{JHM} and rJHM/N_{A59} as well as the parental viruses rA59 and rJHM. Sagittal sections from brains harvested at 5 days postinfection were stained for viral antigen. Brains from rA59/N_{JHM}-infected mice expressed more antigen than those from rA59-infected mice but less than rJHM-infected mice (Fig. 5A). Similar to infection with rA59/N_{JHM} and as expected (15, 40), rA59/S_{JHM}-infected mice displayed levels of antigen intermediate between infections with parental rA59 and rJHM (Fig. 5A). When JHM S and N genes are both expressed in rA59/S_{JHM}/N_{JHM}, the virus expresses antigen to an even greater extent, closer to that observed for rJHM (Fig. 5A). These observations were confirmed by quantification of antigen staining, carried out using Image Pro software as described in Materials and Methods (Fig. 5C). A similar pattern was observed in spread of the JHM background viruses. The extent of antigen was reduced in brain sections from rJHM/N_{A59}-infected mice compared to those from rJHM-infected mice, and the extent of antigen observed in sections from rJHM/S_{A59}-infected mice was reduced further (Fig. 5B and D). Finally, sections from mice infected with rJHM/S_{A59}/N_{A59} had even less antigen expression, similar to rA59-infected mice (Fig. 5B and D).

Exchange of nucleocapsid protein in A59/JHM chimeric viruses does not affect spread of MHV in primary neuronal cultures. To begin to understand the mechanism by which JHM N enhances neurovirulence and spread in the CNS *in vivo*, we tested the hypothesis that JHM N may enhance the

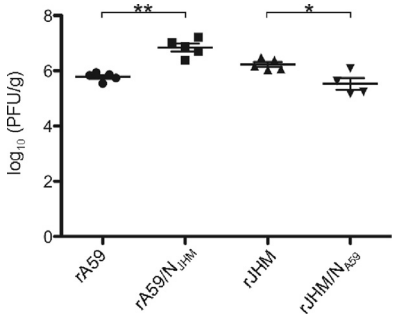

FIG. 4. Replication of chimeric viruses in the brain. C57BL/6 mice (four or more per virus) were inoculated i.c. with 50 PFU of the indicated viruses. At 5 days postinfection mice were sacrificed, and virus titers from brain lysates were determined by plaque assay on L2 cells. Symbols represent individual animals, and the lines represent the mean and the standard error. *, $P = 0.01$; **, $P = 0.0001$. Data are from one representative experiment of two or more.

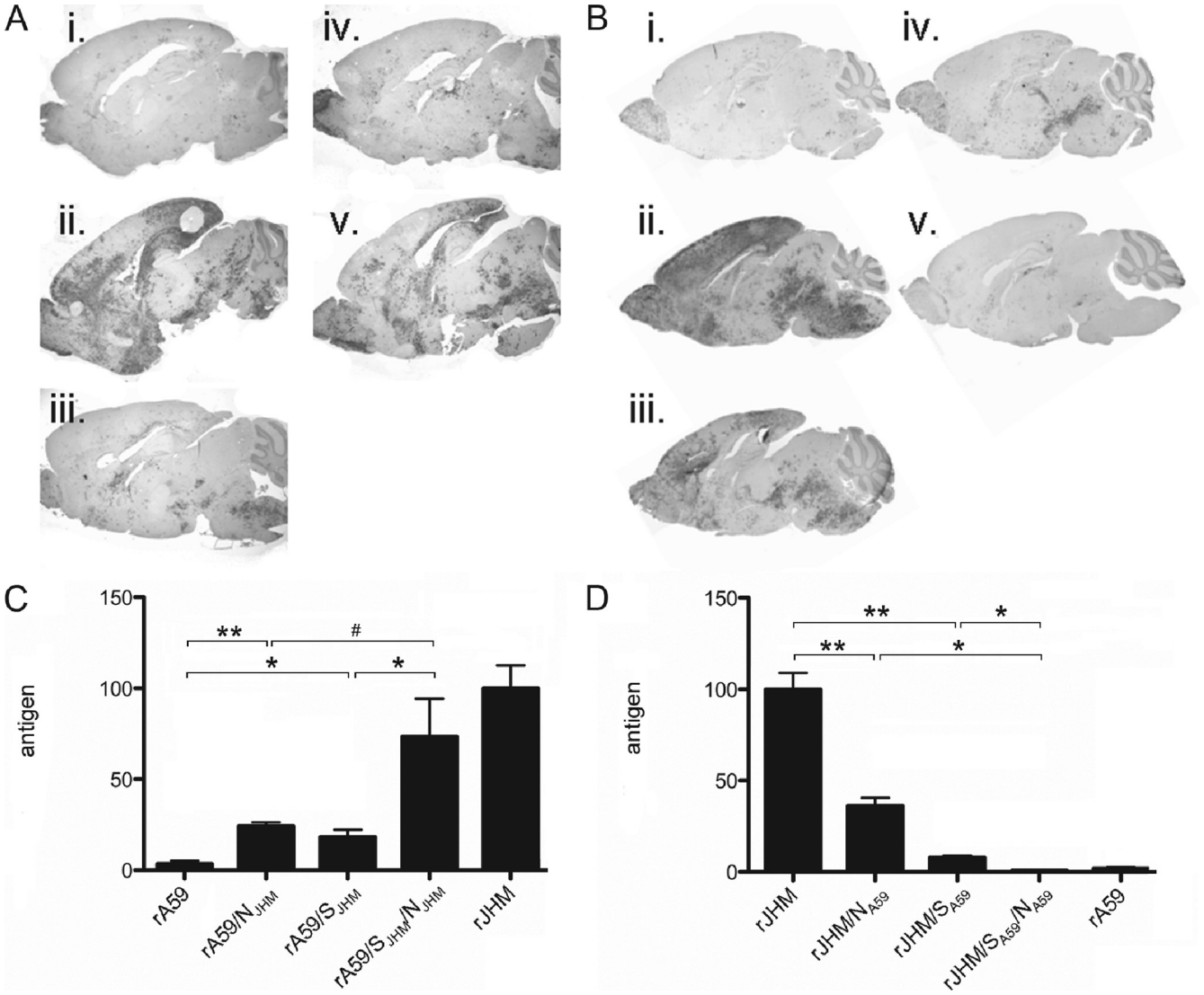

FIG. 5. Viral antigen expression in the brains of infected mice. C57BL/6 mice were inoculated i.c. with 50 PFU of virus and sacrificed at 5 days postinfection. Brains were harvested, sectioned sagitally, and stained for viral antigen expression with anti-N MAb as described in Materials Methods. (A) Frame i, rA59; frame ii, rJHM; frame iii, rA59/N_{JHM}; frame iv, rA59/S_{JHM}; frame v, rA59/S_{JHM}//N_{JHM}. (B) Frame i, rA59; frame ii, JHM; frame iii, rJHM/N_{A59}; frame iv, rJHM/S_{A59}; frame v, rJHM/S_{A59}/N_{A59}. Panels C (A59 background viruses from panel A) and D (JHM background viruses from panel B) show quantification of antigen staining using the color-cubed segmentation function of Image Pro, version 5.0, software. The *y* axis represents the area of antigen stain relative to rJHM, which is set to 100. Data shown represent the mean and standard error and are from one representative of two or more experiments. *, $P < 0.05$; **, $P \leq 0.0001$; #, $P = 0.08$.

ability to spread among neurons, the major CNS cell type infected by both JHM and A59 (8, 28) (unpublished data). JHM N was found to be closely associated with microtubules in the rat neuronal cell line OBL-21 and to share homology with microtubule binding protein, tau; this implies a possible role of N in microtubule transport and spread (39). Thus, we compared the spread of wild-type viruses and N exchange chimeras in primary neuronal cultures by examining the sizes of discrete infected foci (Fig. 6A). We had previously observed that rA59 and rJHM initially produced similar numbers of infected foci in primary neurons but that, by 24 to 48 h postinfection, the rJHM-infected cultures have larger numbers of cells per focus (unpublished data). Neurons were infected at an MOI of 1 with rA59/N_{JHM} and rJHM/N_{A59} along with control viruses rA59 and rJHM, and cultures were fixed and stained with MAb for N expression at 1 and 3 days postinfection (Fig. 6A) or 2 and 4 days postinfection (Fig. 6B). (The rA59- and rA59/N_{JHM}-infected cultures were assayed at later times because the infection spreads more slowly than in rJHM-infected cultures). No obvious differences in spread were observed; isolated foci of rA59/N_{JHM}-infected cells were similar in size to those generated by infection with rA59, and foci of rJHM/N_{A59}-infected cells were similar in size to those generated by rJHM infection (Fig. 6A and B). Quantification of the area of antigen staining per focus using Image Pro software confirmed that there were no significant differences in *in vitro* spread between isogenic viruses differing only in N (Fig. 6C and D). It has previously been observed that expression of JHM S within the A59 back-

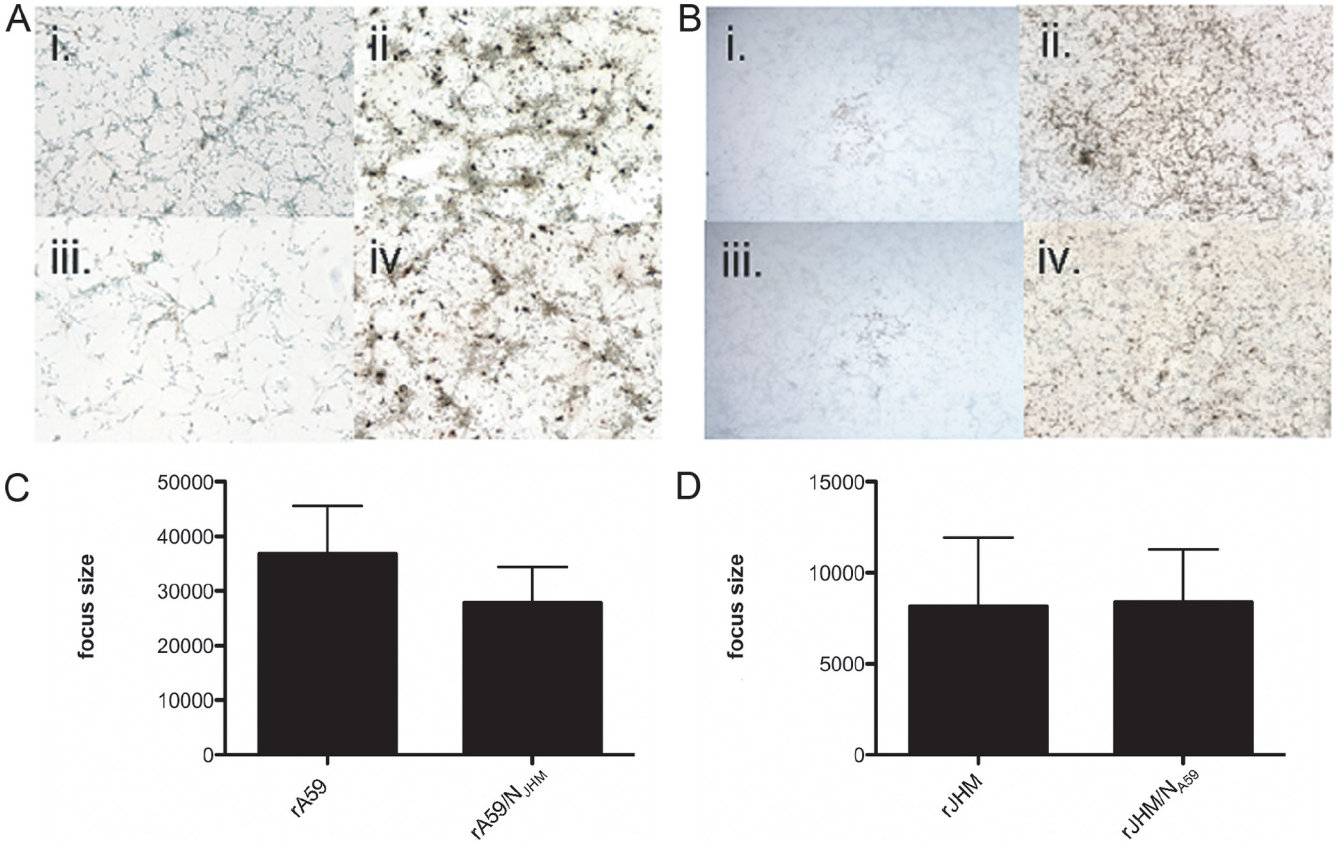

FIG. 6. Virus spread in primary neuronal cultures. Neuronal cultures were infected with recombinant viruses as indicated at an MOI of 1 and were fixed and stained with anti-N MAb using immunoperoxidase at the times postinfection as indicated. (A) frame i, rA59 at 2 days postinfection (dpi) (magnification, ×20); frame ii, rA59 at 4 dpi (×20); frame iii, rA59/N_{JHM} at 2 dpi (×20); frame iv, rA59/N_{JHM} at 4 dpi (×20). (B) Frame i, rJHM at 1 dpi (×4); frame ii, rJHM at 3 dpi (×4); frame iii, rJHM/N_{A59} at 1 dpi (×4); frame iv, rJHM/N_{A59} at 3 dpi (×4). (C and D) Quantification of neuronal spread for A59 background viruses (C) and JHM background viruses (D) using the color-cubed segmentation function of Image Pro, version 5.0, software. The *y* axis shows arbitrary units that represent the average area of infection foci; differences in scales between panels C and D are due to differences in magnifications of analyzed photos. Data shown represent the mean and standard error and are from one representative experiment of five.

ground conferred enhanced spread in primary neuronal cultures as measured by the numbers of cells per infected focus (41). When JHM S and N were expressed together in the A59 background, N did not enhance spread (data not shown). Thus, while expression of JHM N within the A59 background does seem to enhance CNS spread *in vivo*, this does not appear to be due to an inherent ability to spread more rapidly among neurons.

Induction of a robust CNS T-cell response by MHV is modified by the exchange of A59 and JHM nucleocapsid genes. rA59 infection induces a strong CD8 T-cell response in the CNS, and this response is crucial for clearance of virus (12, 22). In contrast, the CD8 T-cell response against rJHM in the CNS is minimal (15, 21, 43). The lack of an effective CD8 T-cell response likely contributes to the high neurovirulence of JHM. Interestingly, the extent of the CD8 T-cell response is not dependent on the S gene but, rather, on one or more background gene(s), as evidenced by the finding that rA59/S_{JHM} induces an even stronger T-cell response than rA59 while rJHM/S_{A59}, like rJHM, fails to induce a significant T-cell response (15, 21). We used the N exchange chimeric viruses to investigate whether N protein is a determinant of the extent of T cell response in the CNS.

For studies of CD8 T-cell response, we compared N exchange viruses to isogenic parental viruses. Initially, we used as parental controls viruses expressing the JHM S because the immunodominant MHV CD8 T-cell epitope, S510 (H-2^b), is not expressed by the A59 S protein, and we wanted to compare viruses with the same CD8 T-cell epitopes. Mice were infected i.n. with 500 PFU of rJHM/N_{A59} or rJHM and, as a positive control for CD8 T-cell response, rA59/S_{JHM}. At 7 days postinfection brain mononuclear cells were isolated and stained for expression of CD3-, CD4-, CD8-, and S510-specific T-cell receptors. Flow cytometry was used to determine the percentage of CD4, CD8, and S510 epitope-specific CD8 T cells within each sample, and the T-cell numbers per brain were calculated by multiplying the percentages of CD8, CD4, and specific CD8 T cells by the total number of cells isolated from each brain (Fig. 7A). The T-cell response (both CD8 and CD4) to rJHM/N_{A59} was significantly greater than the response to rJHM but less than that to rA59/S_{JHM}. Thus, JHM N was required in order for the T-cell response against the virus to be weak.

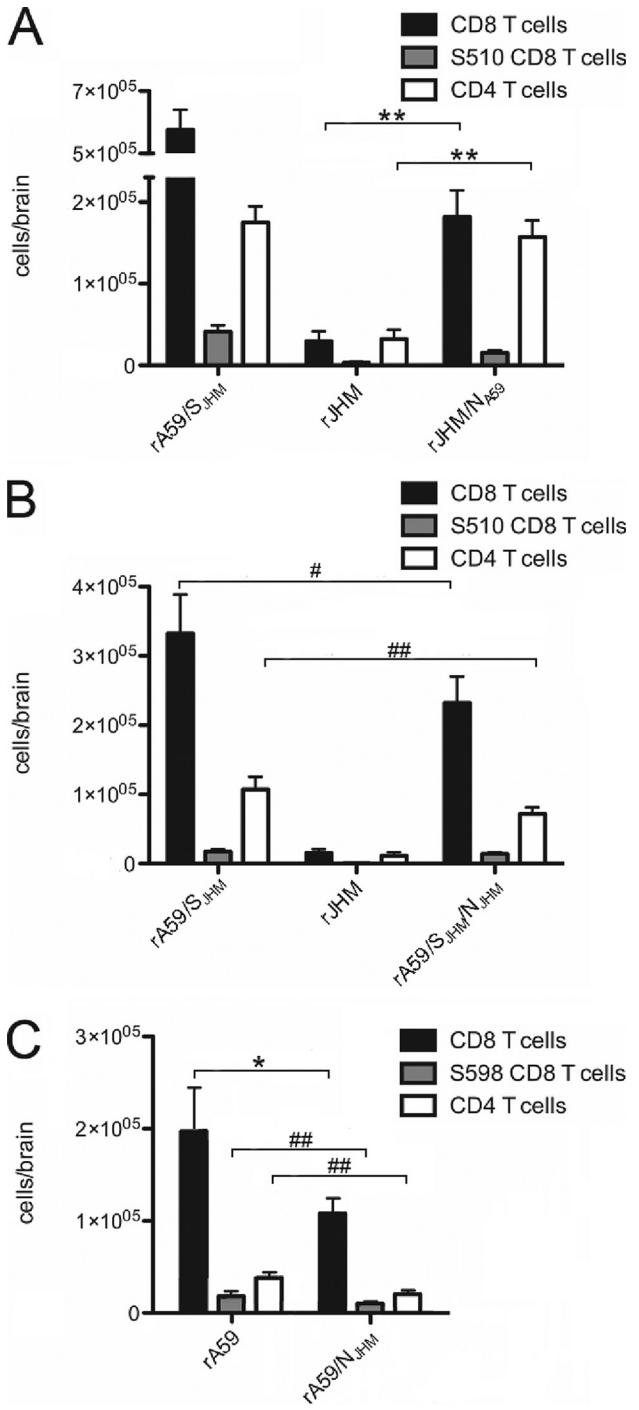

FIG. 7. T-cell response to recombinant viruses in the brain. Mice were infected with recombinant viruses and sacrificed at 7 days postinfection. Mononuclear cells were isolated from the brains of infected animals, stained with T-cell type-specific antibodies and either S510-specific tetramers (A and B) or assayed for secretion of IFN-γ in response to S598 peptide (C), and analyzed by flow cytometry as described in Materials and Methods. The total number of each T-cell population in the brain was determined by multiplying the percentage of each cell type by the total number of cells isolated per brain. Shown are the means and standard errors for the total CD8 T, epitope-specific CD8 T, and CD4 T cells in the brains of mice infected with rJHM/N_{A59}, rA59/S_{JHM}, and rJHM (A); rA59/S_{JHM}/N_{JHM}, rA59/S_{JHM}, and rJHM (B); and rA59 and rA59/N_{JHM} (C). *, $P < 0.05$; **, $P \leq 0.0005$; #, $P = 0.15$; ##, $P \leq 0.09$. Each panel is representative of at least two experiments.

Similar analyses of the reciprocal JHM background viruses were carried out to investigate whether expression of the JHM nucleocapsid in the A59 background confers a less robust T-cell response phenotype. Mice were infected with rA59/S_{JHM}/N_{JHM}, rA59/S_{JHM}, and rJHM, and the total numbers of CD8-, CD4-, and S510-specific CD8 T cells in the brains of infected mice were calculated as above (Fig. 7B). Brain mononuclear cells from rA59/S_{JHM}-infected mice contained more CD8-, CD4-, and S510-specific CD8 T cells than those from rA59/S_{JHM}/N_{JHM}-infected mice. Cells from the brains of rJHM-infected mice had, as expected, minimal levels of CD8-, CD4-, and S510-specific CD8 T cells, significantly less than brains of rA59/S_{JHM}-infected mice. Thus, expression of the JHM N did reduce the T-cell response compared with the isogenic parental virus expressing A59 N; however, the difference did not reach statistical significance.

To determine the level of T-cell expression conferred by expression of the JHM N protein alone in the presence of A59 background genes, mice were infected with rA59 and rA59/N_{JHM}, and the total numbers of T cells were quantified as above. Since we were unable to obtain a suitable MHC tetramer reagent for quantification of S598-specific T cells, we quantified S598-specific T cells in the brains of infected animals utilizing an intracellular cytokine staining assay for IFN-γ, following incubation with S598 peptide (Fig. 7C). Brain mononuclear cells from rA59-infected mice contained more total CD8- and S598-specific CD8 T cells than generated by rA59/N_{JHM} infection. As shown in Fig. 7A, the difference in the numbers of total CD8 T cells was statistically significant. Thus, the data in Fig. 7 indicate that expression of the A59 N in the JHM background leads to an increase in the T-cell response while expression of JHM N from within the rA59 genome likely leads to a small reduction in the T-cell response.

Expression of JHM nucleocapsid protein from within the A59 background does not impair the ability of MHV to induce hepatitis. In addition to the striking difference in neurovirulence, rJHM and rA59 differ greatly in ability to infect the liver and cause hepatitis. While rA59 induces moderate hepatitis when inoculated directly into the liver at a dose of 500 PFU, JHM replicates only minimally in the liver even when doses as high as 10^5 PFU are administered. Perhaps surprisingly, analysis of chimeric viruses indicates that the ability to induce hepatitis does not map to the A59 S gene but, rather, to another gene(s) encoded in the 3′ end of the genome (31). In addition, the N genes of some MHV strains were shown to be responsible for the induction of fgl2, a procoagulant, which was necessary for MHV-3-induced fulminant hepatitis in BALB/c mice (6, 27, 35). Thus, we used the A59/JHM N exchange viruses to further investigate a role for N in replication and virulence in the liver. Mice were infected intrahepatically, a route which induces hepatitis but no CNS infection, with 500 PFU of rA59, rJHM, and rA59/N_{JHM}. Both rA59 and rA59/N_{JHM} replicated to high titers that were significantly greater than the titer of rJHM, which replicated near or below the limit of detection (Fig. 8A). Thus, JHM N expression does not preclude replication in the liver though rA59/N_{JHM} replicated to a slightly but significantly lower titer than rA59 (P value of 0.0015). Replication in the liver of JHM background chimeras rJHM/N_{A59} and rJHM/S_{A59}/N_{A59} was also compared to that of parental rJHM and rA59 (Fig. 8B). Because rJHM replicates to

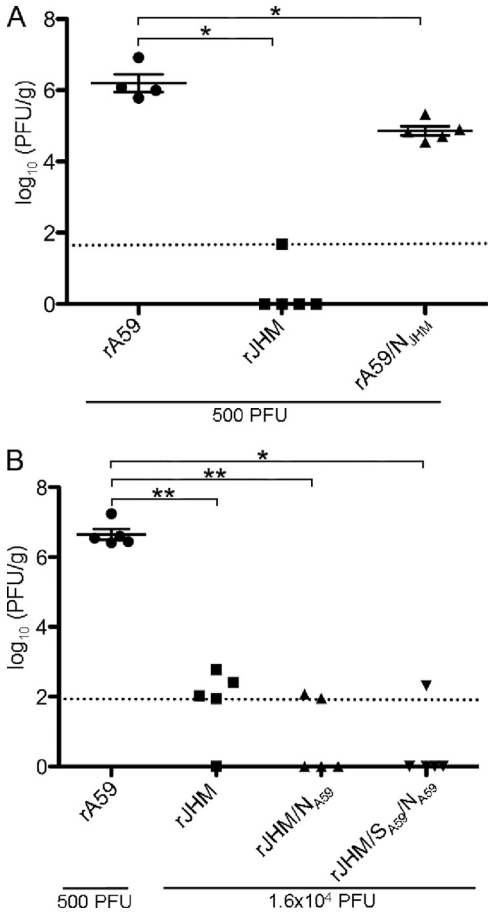

FIG. 8. Replication of chimeric viruses in the liver. C57BL/6 mice were inoculated intrahepatically with viruses at the doses as indicated. Mice were sacrificed at 5 days postinfection, and virus titers were determined from liver lysates. (A) rA59, rJHM, and rA59/N_{JHM} (500 PFU). (B) rA59 (500 PFU) and rJHM, rJHM/N_{A59}, and rJHM/S_{A59}/N_{A59} (1.6×10^4 PFU). Symbols represent individual animals, and the lines represent the mean and the standard error. The dotted lines represent the limits of detection. These data are from one representative experiment of two or more. *, $P < 0.02$; **, $P < 0.0001$.

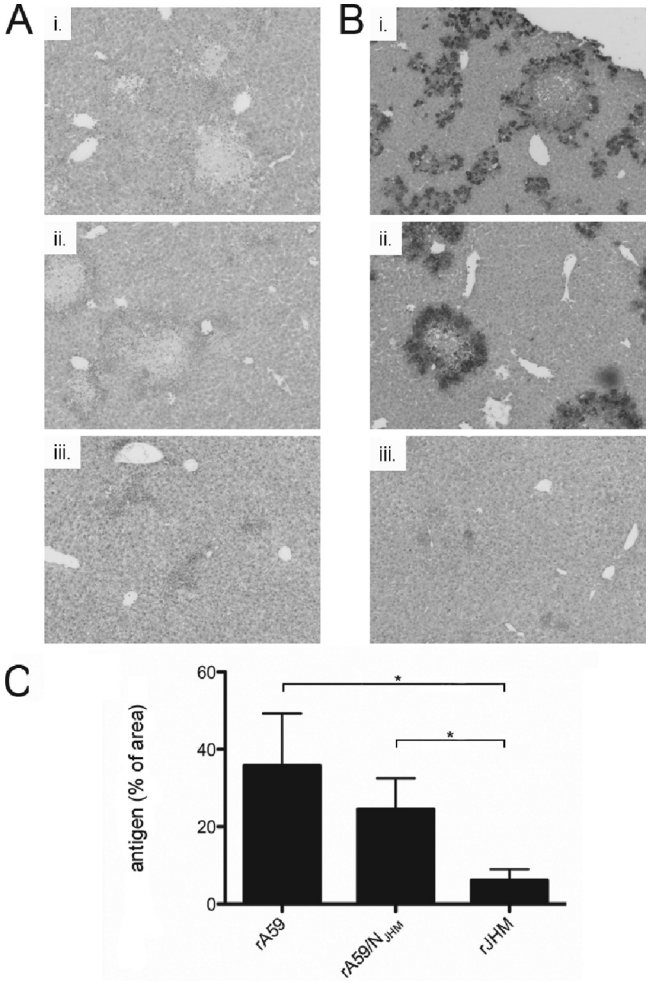

FIG. 9. Pathology and viral antigen expression in the livers of mice infected with chimeric viruses. C57BL/6 mice were inoculated intrahepatically with 500 PFU of rA59 and rA59/N_{JHM} and 1.8×10^4 PFU of rJHM. Mice were sacrificed at 5 days postinfection. Livers were harvested, sectioned, and stained either for pathology or viral antigen expression. (A) Hematoxylin- and eosin-stained sections: frame I, rA59; frame ii, rA59/N_{JHM}; frame iii, rJHM. (B) Immunoperoxidase-stained sections using anti-N MAb: frame i, rA59; frame ii, rA59/N_{JHM}; frame iii, rJHM. (C) Quantification of antigen staining using the color cube-based segmentation function of Image Pro, version 5.0, software. The *y* axis represents the area of antigen stain over total area of the liver section, and values are shown as mean and standard error. The data shown in all panels are representative of four or five mice per group; two adjacent sections were stained per animal. *, $P < 0.05$.

such a minimal extent in the liver, very large inocula (1.8×10^4 PFU) were used. All of the JHM background viruses replicated near or below the limit of detection, despite the difference in amount inoculated. There were no significant differences between rJHM/N_{A59}, rJHM/S_{A59}/N_{A59}, and rJHM in the levels of replication, so neither A59 N nor A59 S and N in combination is able to confer upon rJHM the ability to replicate in the liver.

Liver sections from a similar experiment were analyzed for degree of hepatitis and viral antigen expression. To quantify hepatitis, sections were stained with hematoxylin and eosin, observed for necrosis and immune infiltration, and blindly scored for hepatitis severity, using a four-unit scoring scale (4, severe; 3, moderate; 2, mild; 1, minimal) (3, 31). Liver sections from rA59- and rA59/N_{JHM}-infected mice displayed moderate to severe hepatitis, with average scores of 3.75 and 3.31, respectively (Fig. 9A). The levels of hepatitis were similar for infections with rA59 and rA59/N_{JHM}, indicating that in the context of A59/JHM chimeras, N is not an important determinant of hepatovirulence. Sections from mice infected with a very high dose of rJHM (approximately 35-fold more than the other viruses) displayed little visible damage; however, they did exhibit some inflammation (Fig. 9A). To measure viral antigen, sections were immunoperoxidase stained using anti-N MAb as above (Fig. 9B). Sections from both rA59- and rA59/N_{JHM}-infected mice had extensive staining, with rA59 sections showing slightly more antigen. Minimal staining was observed in liver sections from mice that had been inoculated with a high dose of rJHM. Image Pro software was utilized to measure the extent of viral antigen staining. Antigen levels in the liver from rA59/N_{JHM}-infected mice were not significantly different from

those of rA59-infected mice while livers from rJHM-infected mice, as expected, had minimal levels of viral antigen (Fig. 9C).

DISCUSSION

The availability of a reverse genetics system for MHV and the selection and characterization of A59/JHM chimeric recombinant viruses have allowed us to begin to map the viral genes responsible for the strain-specific differences in pathogenesis. Previous studies of chimeric A59/JHM recombinant viruses indicated that (i) the JHM S is a determinant of neurovirulence, but not the only determinant (40); (ii) other viral genes encoded in the 3′ portion of the genome contribute significantly to the extensive antigen spread in the CNS and high mortality induced by JHM (15, 23, 31, 40); and (iii) the ability to induce hepatitis maps not to the A59 spike but, rather, to other genes encoded in the 3′ portion of the viral genome (31, 32). Because of the multifunctional nature of N protein, with roles as a structural protein and in replication, we chose to examine the role of N in pathogenesis. Thus, we selected and characterized A59/JHM chimeric viruses in which the N genes were exchanged. The ability to obtain clear answers in mapping pathogenic properties both in our previous studies (31, 32, 40) and in the studies described herein indicates that the use of chimeric viruses is not generally compromised by phenotypes that may be due to interactions of heterologous proteins.

When N exchange recombinant viruses were compared to their respective parental wild-type viruses, there were no major differences observed in plaque morphology (data not shown) or in replication in L2 cells (Fig. 2A). In contrast, *in vivo* differences were striking. JHM N, when expressed within the A59 background (rA59/N_{JHM}), conferred enhanced virulence, as evidenced by an LD_{50} approximately 1,000-fold lower than that of rA59. The reverse exchange viruses showed a similar but less dramatic result; expression of A59 N within the JHM background (rJHM/N_{A59}) slightly increased survival time compared to infection with rJHM (Fig. 2B). It is difficult to measure differences in virulence between these two highly neurovirulent viruses. Attenuation conferred by expression of A59 N in the JHM background was more easily observed in a comparison of rJHM/S_{A59}/N_{A59} and the already attenuated rJHM/S_{A59} (Fig. 2D).

The differences in neurovirulence observed in N exchange viruses compared with wild-type isogenic viruses were reflected in the small but statistically significant differences in replication in the CNS after i.c. inoculation (Fig. 4). More strikingly, expression of JHM N within the A59 background conferred increased antigen expression in the brain while reciprocal expression of A59 N within the JHM background conferred a decrease in the level of antigen expression in the brain (Fig. 5A to D). In agreement with previous studies from our lab, the level of MHV antigen expression in the brain is a consistent correlate of virulence (15, 41).

We considered several possible mechanisms to explain the differences in neurovirulence and antigen spread in the brain between N exchange viruses. (i) Expression of JHM N could confer an ability to spread among neurons more efficiently or expand the tropism of the virus for more neuronal subtypes. (ii) JHM N expression could enhance spread among glial cells or between glial cells and neuronal cells; this seemed unlikely as no differences in spread were observed in primary astrocyte cultures (data not shown). (iii) JHM N could alter the immune response, allowing greater spread than that of parental rA59 strain. The rA59 strain is cleared by a robust CD8 T-cell response (12, 22), and we observed previously that this property mapped within the 3′ end of the genome but not to the JHM spike (21). This left the possibility that N may be responsible for differences in T-cell response.

In order to explore the mechanism by which expression of JHM N enhances the amount of antigen expression in the brain, we examined spread in primary hippocampal neuronal cultures. Previous studies of A59/JHM chimeric viruses demonstrated that expression of JHM S within the A59 background enhances *in vitro* neuron-to-neuron spread (41) but not to the extent of spread with rJHM (unpublished data). This suggested the possibility that another viral protein could play a role in neuron-to-neuron spread. It had previously been reported that JHM N is closely associated with microtubules in the infected rat neuronal cell line OBL-21 and that N shows strong homology to microtubule binding protein tau (39). This suggested that N could be playing an important role in trafficking of the virus, and we hypothesized that the JHM N may be optimized for fast axonal transport relative to A59 N. However, exchange of N genes failed to confer a measurable difference in spread among primary hippocampal neurons (Fig. 6A to D), implying that the mechanism by which JHM N enhances antigen distribution in the brain is not through enhanced neuron-to-neuron spread. While there are no data indicating that there are any qualitative differences in the types of neurons in the brain infected by JHM compared to A59, we have used only hippocampus-derived neurons, and it is possible that JHM infects a wider range of types of neurons than A59.

To determine if the difference in the ability to induce a robust T-cell response in the CNS maps to the N gene, we compared the T-cell response of N exchange viruses with the isogenic parental viruses rA59 and rA59/S_{JHM}, which induce robust virus-specific T-cell responses, and with rJHM, which induces a very minimal response. Infection with rJHM/N_{A59} resulted in an increased T-cell response in the brain relative to isogenic rJHM, suggesting that JHM nucleocapsid expression is required for the minimal T-cell response phenotype of JHM (Fig. 7A). There was a statistically significant difference in both CD8 and CD4 T-cell numbers. The resulting T-cell response, however, was consistently lower than that of rA59/S_{JHM}, suggesting that although JHM N contributes to the weak T-cell response phenotype, other proteins in the JHM background are likely to be important as well (Fig. 7A). Exchange of N genes in the A59 background viruses showed a reciprocal effect. Infection with rA59/$S_{JHM}N_{JHM}$ resulted in a small decrease in the induced T-cell response compared to infection with isogenic rA59/S_{JHM} and an increase over the response to rJHM (Fig. 7B); similarly, the total CD8 T-cell response induced by rA59/N_{JHM} was statistically significantly less than that induced by rA59 infection (Fig. 7C).Thus, while the genotype of N appears to have a modest effect on the T-cell response to MHV infection, it is unlikely that this is the primary mechanism by which JHM N confers increased virulence when expressed in the A59 background.

Differences in the type I IFN response could also play a role

in the virulence associated with JHM N. A59 N was shown to serve as a type I IFN antagonist when expressed from a recombinant ΔE3L vaccinia virus (51), and infection of type I IFN receptor-deficient mice ($IFNAR^{-/-}$) demonstrated that type I IFN is crucial for defense during early infection with A59 and JHM *in vivo* (4, 16, 44). Thus, it is possible that JHM N could be a more potent IFN antagonist than A59 N and thus compromise host defenses. However, this is unlikely, as supported by the following observations: rA59 and rJHM induced similar levels of type I IFN in the brains of infected mice, and both strains were significantly more lethal in $IFNAR^{-/-}$ mice than in wild-type isogenic mice (44). In the absence of a type I IFN response, rJHM is able to spread from the brain into the periphery and replicate in the liver as well as in other organs not usually infected by JHM (16, 44), underscoring the inability of JHM to overcome the antiviral state induced by IFN in wild-type mice. Furthermore, there were no differences in the ability of A59 and JHM to induce type I IFN in fibroblasts or in macrophages or to replicate in L2 cells (45) or macrophages (unpublished) that were pretreated with IFN-β.

In addition to the differences in neurovirulence, A59 and JHM vary greatly in their ability to replicate in the liver and cause hepatitis. The ability of A59 to replicate to high titers in the liver and cause severe hepatitis does not map to the S gene but, rather, to one or more other genes in the 3′ end of the A59 genome (31). The studies presented here clearly show that the ability to induce hepatitis in C57BL/6 mice, in the context of A59/JHM chimeras, does not depend on the N gene of the A59 strain and that expression of the N and S genes of A59 within the JHM background is not sufficient to induce hepatitis (Fig. 8B). Though replacing the A59 N gene with that of JHM did not prevent the virus from causing severe hepatitis, expressing JHM N in the A59 background did significantly reduce viral liver titers by about 10-fold at 5 days postinfection (Fig. 8A) and caused slight, though insignificant, decreases in hepatitis and viral antigen expression in the liver (Fig. 9A to C). Thus, although expression of JHM N clearly does not block MHV-induced hepatitis, expression of JHM N may play a minor role in decreasing the level of replication in the liver. Levy and colleagues demonstrated that the highly hepatotropic strains MHV-3 and A59 (but not the nonheptatotropic JHM strain) induce fibrinogen-like protein 2 (fgl2) and that fgl2 induction is responsible for the induction of fulminant hepatitis in MHV-3-infected mice (6, 35). Interestingly, the induction of fgl2 was mapped to the N protein of hepatotropic strains (35). However, in the studies presented here, replacement of the N gene of A59 with that of the nonhepatotropic JHM did not prevent the resulting virus ($rA59/N_{JHM}$) from causing severe hepatitis. This demonstrates that in the context of A59/JHM chimeras, the induction of hepatitis does not depend on the N gene of the hepatotropic A59.

It is important to note that the A59 N gene contains within it another gene, in the +1 reading frame, encoding the internal, or I, protein. The I protein is a mostly hydrophobic 23-kDa structural protein of unknown function (9). Interestingly while I protein is expressed by most MHV strains, the JHM strain does not encode the I protein (9, 38). Thus, the I gene could possibly be responsible for one or more of the properties attributed to N including the pathogenic differences between A59 and JHM. However, the data presented here demonstrate that expression of the I gene from within the JHM genome ($rJHM/N_{A59}$) is not sufficient to confer the ability to induce hepatitis. Furthermore, the I gene is unlikely to be an important determinant of pathogenesis as an internal gene knockout recombinant A59 replicated similarly to an isogenic wild-type virus *in vivo*, and no major differences in clinical signs were reported (9).

The data presented here demonstrate that the N gene plays a major role in the extent of neurovirulence and a minor role, if any, in MHV-induced hepatitis. While we have not defined the mechanisms by which the N gene influences pathogenic outcome, the data do, however, suggest that increased neurovirulence associated with expression of the JHM N gene within the A59 background is not a result of enhanced neuron-to-neuron spread. The data furthermore indicate that there may be an influence of N on the induction of a robust T-cell response, which is crucial to virus clearance in the CNS. Future studies will be directed at further understanding the differences in virus-host interactions between chimeric and isogenic wild-type viruses. This will focus on the cytokines elicited in response to MHV and how the spread of virus within the CNS affects the host immune response.

ACKNOWLEDGMENTS

This work was supported by NIH grants NS-54695 and AI-60021 to S.R.W. T.J.C. was partially supported by NIH training grant AI-07324.

We thank the members of the Weiss lab for critically reading the manuscript and Sarah Radcliffe for help with the statistics.

REFERENCES

1. **Armstrong, J., S. Smeekens, and P. Rottier.** 1983. Sequence of the nucleocapsid gene from murine coronavirus MHV-A59. Nucleic Acids Res. **11:** 883–891.
2. **Baric, R. S., G. W. Nelson, J. O. Fleming, R. J. Deans, J. G. Keck, N. Casteel, and S. A. Stohlman.** 1988. Interactions between coronavirus nucleocapsid protein and viral RNAs: implications for viral transcription. J. Virol. **62:** 4280–4287.
3. **Batts, K. P., and J. Ludwig.** 1995. Chronic hepatitis. An update on terminology and reporting. Am. J. Surg. Pathol. **19:**1409–1417.
4. **Cervantes-Barragan, L., R. Zust, F. Weber, M. Spiegel, K. S. Lang, S. Akira, V. Thiel, and B. Ludewig.** 2007. Control of coronavirus infection through plasmacytoid dendritic-cell-derived type I interferon. Blood **109:**1131–1137.
5. **Dalziel, R. G., P. W. Lampert, P. J. Talbot, and M. J. Buchmeier.** 1986. Site-specific alteration of murine hepatitis virus type 4 peplomer glycoprotein E2 results in reduced neurovirulence. J. Virol. **59:**463–471.
6. **Ding, J. W., Q. Ning, M. F. Liu, A. Lai, K. Peltekian, L. Fung, C. Holloway, H. Yeger, M. J. Phillips, and G. A. Levy.** 1998. Expression of the fgl2 and its protein product (prothrombinase) in tissues during murine hepatitis virus strain-3 (MHV-3) infection. Adv. Exp. Med. Biol. **440:**609–618.
7. **Fan, H., A. Ooi, Y. W. Tan, S. Wang, S. Fang, D. X. Liu, and J. Lescar.** 2005. The nucleocapsid protein of coronavirus infectious bronchitis virus: crystal structure of its N-terminal domain and multimerization properties. Structure **13:**1859–1868.
8. **Fazakerley, J. K., S. E. Parker, F. Bloom, and M. J. Buchmeier.** 1992. The V5A13.1 envelope glycoprotein deletion mutant of mouse hepatitis virus type-4 is neuroattenuated by its reduced rate of spread in the central nervous system. Virology **187:**178–188.
9. **Fischer, F., D. Peng, S. T. Hingley, S. R. Weiss, and P. S. Masters.** 1997. The internal open reading frame within the nucleocapsid gene of mouse hepatitis virus encodes a structural protein that is not essential for viral replication. J. Virol. **71:**996–1003.
10. **Goebel, S. J., B. Hsue, T. F. Dombrowski, and P. S. Masters.** 2004. Characterization of the RNA components of a putative molecular switch in the 3′ untranslated region of the murine coronavirus genome. J. Virol. **78:**669–682.
11. **Gombold, J. L., S. T. Hingley, and S. R. Weiss.** 1993. Fusion-defective mutants of mouse hepatitis virus A59 contain a mutation in the spike protein cleavage signal. J. Virol. **67:**4504–4512.
12. **Gombold, J. L., R. M. Sutherland, E. Lavi, Y. Paterson, and S. R. Weiss.** 1995. Mouse hepatitis virus A59-induced demyelination can occur in the absence of CD8+ T cells. Microb. Pathog. **18:**211–221.
13. **Huang, Q., L. Yu, A. M. Petros, A. Gunasekera, Z. Liu, N. Xu, P. Hajduk, J. Mack, S. W. Fesik, and E. T. Olejniczak.** 2004. Structure of the N-terminal

RNA-binding domain of the SARS CoV nucleocapsid protein. Biochemistry **43:**6059–6063.

14. **Hurst, K. R., L. Kuo, C. A. Koetzner, R. Ye, B. Hsue, and P. S. Masters.** 2005. A major determinant for membrane protein interaction localizes to the carboxy-terminal domain of the mouse coronavirus nucleocapsid protein. J. Virol. **79:**13285–13297.
15. **Iacono, K. T., L. Kazi, and S. R. Weiss.** 2006. Both spike and background genes contribute to murine coronavirus neurovirulence J. Virol. **80:**6834–6843.
16. **Ireland, D. D., S. A. Stohlman, D. R. Hinton, R. Atkinson, and C. C. Bergmann.** 2008. Type I interferons are essential in controlling neurotropic coronavirus infection irrespective of functional CD8 T cells. J. Virol. **82:**300–310.
17. **Jayaram, H., H. Fan, B. R. Bowman, A. Ooi, J. Jayaram, E. W. Collisson, J. Lescar, and B. V. Prasad.** 2006. X-ray structures of the N- and C-terminal domains of a coronavirus nucleocapsid protein: implications for nucleocapsid formation. J. Virol. **80:**6612–6620.
18. **Kuo, L., G. J. Godeke, M. J. Raamsman, P. S. Masters, and P. J. Rottier.** 2000. Retargeting of coronavirus by substitution of the spike glycoprotein ectodomain: crossing the host cell species barrier. J. Virol. **74:**1393–1406.
19. **Lavi, E., D. H. Gilden, M. K. Highkin, and S. R. Weiss.** 1984. Persistence of mouse hepatitis virus A59 RNA in a slow virus demyelinating infection in mice as detected by in situ hybridization. J. Virol. **51:**563–566.
20. **Lavi, E., D. H. Gilden, Z. Wroblewska, L. B. Rorke, and S. R. Weiss.** 1984. Experimental demyelination produced by the A59 strain of mouse hepatitis virus. Neurology **34:**597–603.
21. **MacNamara, K. C., S. J. Bender, M. M. Chua, R. Watson, and S. R. Weiss.** 2008. Priming of $CD8^+$ T cells during central nervous system infection with a murine coronavirus is strain-dependent. J. Virol. **82:**6150–6160.
22. **MacNamara, K. C., M. M. Chua, P. T. Nelson, H. Shen, and S. R. Weiss.** 2005. Increased epitope-specific CD8+ T cells prevent murine coronavirus spread to the Spinal Cord and Subsequent Demyelination. J. Virol. **79:**3370–3381.
23. **MacNamara, K. C., M. M. Chua, J. J. Phillips, and S. R. Weiss.** 2005. Contributions of the viral genetic background and a single amino acid substitution in an immunodominant CD8+ T-cell epitope to murine coronavirus neurovirulence. J. Virol. **79:**9108–9118.
24. **Marten, N. W., S. A. Stohlman, R. D. Atkinson, D. R. Hinton, J. O. Fleming, and C. C. Bergmann.** 2000. Contributions of CD8+ T cells and viral spread to demyelinating disease. J. Immunol. **164:**4080–4088.
25. **Masters, P. S.** 1992. Localization of an RNA-binding domain in the nucleocapsid protein of the coronavirus mouse hepatitis virus. Arch. Virol. **125:**141–160.
26. **Matthews, A. E., S. R. Weiss, and Y. Paterson.** 2002. Murine hepatitis virus—a model for virus-induced CNS demyelination. J. Neurovirol. **8:**76–85.
27. **McGilvray, I. D., Z. Lu, A. C. Wei, A. P. Dackiw, J. C. Marshall, A. Kapus, G. Levy, and O. D. Rotstein.** 1998. Murine hepatitis virus strain 3 induces the macrophage prothrombinase *fgl-2* through p38 mitogen-activated protein kinase activation. J. Biol. Chem. **273:**32222–32229.
28. **Miura, T. A., E. A. Travanty, L. Oko, H. Bielefeldt-Ohmann, S. R. Weiss, N. Beauchemin, and K. V. Holmes.** 2008. The spike glycoprotein of murine coronavirus MHV-JHM mediates receptor-independent infection and spread in the central nervous system of $Ceacam1a^{-/-}$ mice. J. Virol. **82:**755–763.
29. **Murali-Krishna, K., J. D. Altman, M. Suresh, D. J. Sourdive, A. J. Zajac, J. D. Miller, J. Slansky, and R. Ahmed.** 1998. Counting antigen-specific CD8 T cells: a reevaluation of bystander activation during viral infection. Immunity **8:**177–187.
30. **Navas, S., S. H. Seo, M. M. Chua, J. D. Sarma, E. Lavi, S. T. Hingley, and S. R. Weiss.** 2001. Murine coronavirus spike protein determines the ability of the virus to replicate in the liver and cause hepatitis. J. Virol. **75:**2452–2457.
31. **Navas, S., and S. R. Weiss.** 2003. Murine coronavirus-induced hepatitis: JHM genetic background eliminates A59 spike-determined hepatotropism. J. Virol. **77:**4972–4978.
32. **Navas-Martin, S., M. Brom, M. M. Chua, R. Watson, Z. Qiu, and S. R. Weiss.** 2007. Replicase genes of murine coronavirus strains A59 and JHM are interchangeable: differences in pathogenesis map to the 3′ one third of the genome. J. Virol. **81:**1022–1026.
33. **Navas-Martin, S., M. Brom, and S. R. Weiss.** 2006. Role of the replicase gene of the murine coronavirus JHM strain in hepatitis. Adv. Exp. Med. Biol. **581:**415–420.
34. **Nelson, G. W., and S. A. Stohlman.** 1993. Localization of the RNA-binding domain of mouse hepatitis virus nucleocapsid protein. J. Gen. Virol. **74:**1975–1979.
35. **Ning, Q., M. Liu, P. Kongkham, M. M. Lai, P. A. Marsden, J. Tseng, B. Pereira, M. Belyavskyi, J. Leibowitz, M. J. Phillips, and G. Levy.** 1999. The nucleocapsid protein of murine hepatitis virus type 3 induces transcription of the novel *fgl2* prothrombinase gene. J. Biol. Chem. **274:**9930–9936.
36. **Ontiveros, E., T. S. Kim, T. M. Gallagher, and S. Perlman.** 2003. Enhanced virulence mediated by the murine coronavirus, mouse hepatitis virus strain JHM, is associated with a glycine at residue 310 of the spike glycoprotein. J. Virol. **77:**10260–10269.
37. **Ontiveros, E., L. Kuo, P. S. Masters, and S. Perlman.** 2001. Inactivation of expression of gene 4 of mouse hepatitis virus strain JHM does not affect virulence in the murine CNS. Virology **289:**230–238.
38. **Parker, M. M., and P. S. Masters.** 1990. Sequence comparison of the N genes of five strains of the coronavirus mouse hepatitis virus suggests a three domain structure for the nucleocapsid protein. Virology **179:**463–468.
39. **Pasick, J. M., K. Kalicharran, and S. Dales.** 1994. Distribution and trafficking of JHM coronavirus structural proteins and virions in primary neurons and the OBL-21 neuronal cell line. J. Virol. **68:**2915–2928.
40. **Phillips, J. J., M. M. Chua, E. Lavi, and S. R. Weiss.** 1999. Pathogenesis of chimeric MHV4/MHV-A59 recombinant viruses: the murine coronavirus spike protein is a major determinant of neurovirulence. J. Virol. **73:**7752–7760.
41. **Phillips, J. J., M. M. Chua, G. F. Rall, and S. R. Weiss.** 2002. Murine coronavirus spike glycoprotein mediates degree of viral spread, inflammation, and virus-induced immunopathology in the central nervous system. Virology **301:**109–120.
42. **Reed, L. J., and H. Muench.** 1938. A simple method of estimating fifty percent points. Am. J. Hyg. **27:**493–497.
43. **Rempel, J. D., S. J. Murray, J. Meisner, and M. J. Buchmeier.** 2004. Differential regulation of innate and adaptive immune responses in viral encephalitis. Virology **318:**381–392.
44. **Roth-Cross, J. K., S. J. Bender, and S. R. Weiss.** 2008. Murine coronavirus mouse hepatitis virus (MHV) is recognized by MDA5 and induces type I IFN in brain macrophages/microglia. J. Virol. **82:**9829–9838.
45. **Roth-Cross, J. K., L. Martinez-Sobrido, E. P. Scott, A. Garcia-Sastre, and S. R. Weiss.** 2007. Inhibition of the IFN-α/β response by mouse hepatitis virus (MHV) at multiple levels. J. Virol. **81:**7189–7199.
46. **Saikatendu, K. S., J. S. Joseph, V. Subramanian, B. W. Neuman, M. J. Buchmeier, R. C. Stevens, and P. Kuhn.** 2007. Ribonucleocapsid formation of severe acute respiratory syndrome coronavirus through molecular action of the N-terminal domain of N protein. J. Virol. **81:**3913–3921.
47. **Spaan, W. J. M., J. Delius, M. A. Skinner, J. Armstrong, P. Rottier, S. Smeekens, B. A. M. van der Zeijst, and S. G. Siddell.** 1983. Coronavirus mRNA synthesis involves fusion of non-contiguous sequences. EMBO J. **2:**1839.
48. **Sturman, L. S., K. V. Holmes, and J. Behnke.** 1980. Isolation of coronavirus envelope glycoproteins and interaction with the viral nucleocapsid. J. Virol. **33:**449–462.
49. **Sussman, M. A., R. A. Shubin, S. Kyuwa, and S. A. Stohlman.** 1989. T-cell-mediated clearance of mouse hepatitis virus strain JHM from the central nervous system. J. Virol. **63:**3051–3061.
50. **Wurm, T., H. Chen, T. Hodgson, P. Britton, G. Brooks, and J. A. Hiscox.** 2001. Localization to the nucleolus is a common feature of coronavirus nucleoproteins, and the protein may disrupt host cell division. J. Virol. **75:**9345–9356.
51. **Ye, Y., K. Hauns, J. O. Langland, B. L. Jacobs, and B. G. Hogue.** 2007. Mouse hepatitis coronavirus A59 nucleocapsid protein is a type I interferon antagonist. J. Virol. **81:**2554–2563.
52. **Yount, B., M. R. Denison, S. R. Weiss, and R. S. Baric.** 2002. Systematic assembly of a full-length infectious cDNA of mouse hepatitis virus strain A59. J. Virol. **76:**11065–11078.
53. **Yu, I. M., M. L. Oldham, J. Zhang, and J. Chen.** 2006. Crystal structure of the severe acute respiratory syndrome (SARS) coronavirus nucleocapsid protein dimerization domain reveals evolutionary linkage between *Coronaviridae* and *Arteriviridae*. J. Biol. Chem. **281:**17134–17139.